**Submitted manuscript entitled:** Global aquifers dominated by fossil groundwaters but vulnerable to modern contamination

**Submitted to:** *Nature Geoscience* **on** *23 February 2017*

**Authors:** Scott Jasechko[1,*], Debra Perrone[2,3], Kevin M. Befus[4], M. Bayani Cardenas[5], Grant Ferguson[6], Tom Gleeson[7], Elco Luijendijk[8], Jeffrey J. McDonnell[9,10,11], Richard G. Taylor[12], Yoshihide Wada[13,14,15,16], James W. Kirchner[17,18,19]

**Author affiliations:**
[1] Department of Geography, University of Calgary, Calgary, Alberta, T2N 4H7, Canada
[2] Water in the West, Stanford University, Stanford, California, 94305, USA
[3] Civil and Environmental Engineering, Stanford University, Stanford, California, 94305, USA
[4] Civil and Architectural Engineering, University of Wyoming, Laramie, Wyoming, 82071, USA
[5] Department of Geological Sciences, The University of Texas at Austin, Austin, Texas, 78712, USA
[6] Department of Civil and Geological Engineering, University of Saskatchewan, Saskatoon, Saskatchewan, S7N 5A9, Canada
[7] Department of Civil Engineering and School of Earth and Ocean Sciences, University of Victoria, Victoria, British Columbia, V8P 5C2, Canada
[8] Geoscience Centre, University of Göttingen, Göttingen, 37077, Germany[9] Global Institute for Water Security, and School of Environment and Sustainability, University of Saskatchewan, Saskatoon, Saskatchewan, S7N 3H5, Canada
[10] School of Geosciences, University of Aberdeen, Aberdeen, Scotland, AB24 3FX UK
[11] Department for Forest Engineering, Resources and Management, Oregon State University, Corvallis, Oregon, 97330, USA
[12] Department of Geography, University College London, London, WC1E 6BT, UK
[13] International Institute for Applied Systems Analysis, Schlossplatz 1, Laxenburg, A-2361, Austria
[14] Department of Physical Geography, Utrecht University, Utrecht, 80115, The Netherlands
[15] NASA Goddard Institute for Space Studies, 2880 Broadway, New York, New York, 10025, USA
[16] Center for Climate Systems Research, Columbia University, 2880 Broadway, New York, New York, 10025, USA
[17] Department of Environmental System Sciences, ETH Zürich, Universitätstrasse 16, CH-8092, Switzerland
[18] Swiss Federal Research Institute WSL, Birmensdorf, CH-8903, Switzerland
[19] Department of Earth and Planetary Science, University of California, Berkeley, California, 94720, USA

***Corresponding author:**
Scott Jasechko
Department of Geography, University of Calgary
2500 University Drive, Calgary, AB, T2N 1N4
Telephone: +1 403 220 5584
Fax: +1 403 282 6561
Email: sjasechk@ucalgary.ca

**Words (abstract):** 194
**Words (main text):** 2323
**Words (methods):** 1118
**Number of figures:** 2
**Number of tables:** 1

**The vulnerability of groundwater supplies to contamination is closely related to their age. Fossil groundwaters that infiltrated prior to the Holocene have been documented in numerous aquifers and are widely assumed to be immune to modern contaminants. However, the global prevalence and vulnerability of fossil groundwater to modern-era pollutants have not been systematically studied. Here we analyse groundwater carbon isotope data ($^{12}C$, $^{13}C$, $^{14}C$) from 6455 wells around the globe. We show that fossil groundwaters comprise a large share (42-85%) of total aquifer storage in the upper 1 km of the crust, and the majority of waters pumped from wells deeper than 250 m. Fossil groundwater resources are often exploited unsustainably, but are thought to be unaffected by current climate variability and modern-era pollutants. However, half of the wells in our study that are dominated by fossil groundwater also contain detectable levels of tritium, indicating the presence of much younger, decadal-age waters. The prevalence of decadal-age waters in wells predominantly pumping fossil groundwater implies that contemporary contaminants may be able to reach deep wells tapping fossil aquifers. Thus, the management of fossil groundwater resources should also consider water quality risk along with sustainable use.**

Global groundwater is an immense resource, storing ~100 times more water than all the world's lakes[1,2], supplying ~40% of the water for global irrigated agriculture[3], and providing drinking water to billions of people around the world. Recent research has evaluated the global depths of both the groundwater table[4] and modern groundwater recharged within the past ~50 years[1], but the global prevalence and distribution of "fossil groundwater" remain unclear. Here we define fossil groundwater as groundwater recharged by precipitation more than ~12,000 years ago, prior to the beginning of the Holocene epoch; we define prevalence as the frequency with

68 which regional well waters contain fossil groundwater. Understanding the global extent and
69 depth of fossil groundwater resources is important because of their distinctive susceptibility to
70 overdraft[5], presumed isolation from surface-borne pollutants[6,7], potential vulnerability to
71 geogenic contaminants[8], and isolation from modern climate variability[9].

72 To calculate the prevalence of fossil groundwater in well waters, we compiled a
73 groundwater carbon isotope ($^{12}C$, $^{13}C$, $^{14}C$) database of 6455 well water samples from around the
74 globe. The continental USA and Europe are overrepresented in our compilation, which is also
75 inevitably biased towards sedimentary basins where groundwater use is common (Supplementary
76 Figs. S1 and S2; Methods). Radiocarbon ($^{14}C$) has a half-life of 5730 years and has been widely
77 used to identify fossil groundwaters[10-18]. Stable carbon isotope ($^{12}C$, $^{13}C$) data were used to
78 correct for the dissolution of carbonate rocks, which are devoid of radiocarbon[19] and thus would
79 otherwise distort $^{14}C$-based fossil groundwater calculations. We estimated fossil groundwater
80 fractions in wells around the world using a recently developed radiocarbon end-member mixing
81 model, which accounts for both radioactive decay and carbonate dissolution for pre- and post-
82 Holocene recharge[20]. Our approach, which estimates the fraction of fossil groundwater in a water
83 sample rather than the sample's average age, is designed to be less vulnerable to the aggregation
84 errors that are known to bias mean groundwater age calculations[21-23]. We plotted depth profiles
85 of fossil groundwater for aquifers around the world, and calculated the depth below which fossil
86 groundwater becomes common (>50% of wells pump some fossil groundwater) or dominant
87 (>50% of wells pump >50% fossil groundwater; Methods). Where tritium ($^{3}H$) data were
88 available (n=5661 well water samples), we determined the fraction of the groundwater sample
89 that recharged more recently than ~1953 by relating groundwater $^{3}H$ concentrations to historical
90 precipitation $^{3}H$ time-series[24] (Methods). The threshold year 1953 was selected because

widespread thermonuclear testing in subsequent years increased precipitation tritium levels by ~5 to ~500 times above local natural background concentrations[24], providing a tracer of recently recharged groundwater (e.g., Ref. 15). For samples with both radiocarbon and tritium data, we calculated the fractions of water that (i) recharged more than ~12 thousand years ago (fossil groundwater), (ii) recharged more recently than the year 1953 (post-1953 groundwater), and (iii) was of an intermediate age, having recharged more recently than ~12 thousand years ago, but before the year 1953.

**Fossil groundwater in global aquifers**

Our global compilation of radiocarbon data shows that fossil groundwater is not an anomaly in the upper 1 km of the crust, but instead is common in wells drilled to depths of more than ~250 m (Figs. 1, 2 and S3). Among all surveyed wells (n=6455; Fig. S3), we find that over half of all wells deeper than 250 m yield groundwater that was mostly (>50%) replenished before the Holocene (i.e., minimum fossil groundwater exceeds 50% for the majority of groundwater samples pumped from wells deeper than 250 m). By contrast, post-1953 groundwater becomes increasingly scarce with depth (Fig. 2). Half of all wells deeper than 40 m pump groundwater that is comprised almost entirely (>90%) of groundwater recharged before 1953 (i.e., maximum post-1953 groundwater is less than 10% for the majority of groundwater samples pumped from deeper than 40 m).

Fossil groundwaters are found throughout several major aquifers that sustain modern irrigated agriculture (Fig. 1), including the North China Plain (at depths >200 m), the Southern Central Valley of California (at depths >260 m), the north, central and south High Plains aquifers of the central USA (at depths >120-280 m), Italy's Emilia-Romagna Plain (at depths >100-300

m) and Hungary's Pannonian Basin (at depths >160-300 m). Among our 62 study aquifers (Fig. 1), we find the range of depths below which fossil groundwaters dominate well waters (i.e., fossil groundwaters comprise >50% of the water pumped from more than half of all deeper samples) has a median of 200 m, an upper-lower quartile range of 115-290 m, and a $10^{th}$-$90^{th}$ percentile range of 70-430 m.

*[Fig. 1 and Fig. 2 about here]*

Assuming that isotopes measured in well waters reflect the isotopic compositions of groundwater stored in aquifers and are not the result of contamination by infiltrated surface water or rainfall (e.g., Refs. 1,5,11-18), our data show that fossil groundwater likely comprises 42-85% of total groundwater in the crust's uppermost 1 km, 31-79% in the uppermost 500 m, and 10-63% in the uppermost 100 m (Fig. 2c). By contrast, post-1953 groundwater comprises only 5-22% of total groundwater in the crust's uppermost 1 km, 6-27% in the uppermost 500 m, and 13-51% in the uppermost 100 m (Fig. 2d). Fossil groundwater storage in the uppermost 1 km of the crust is, therefore, ~1.9 to ~17 times larger than post-1953 groundwater stores. By combining our new global fossil groundwater storage estimate with global porosity data[1], we calculate that of the 12-22 million $km^3$ of unfrozen water stored in the uppermost 1 km of the crust[1] (~85-152 m equivalent depth of a column of water), approximately 5-18 million $km^3$ is fossil groundwater (36-130 m equivalent depth), 0.6-4.6 million $km^3$ is post-1953 groundwater (4-33 m equivalent depth), and less than 8000 $km^3$ is recent rain and snow that becomes streamflow in less than three months[25] (<0.055 m equivalent depth).

Figs. 1 and 2 show that the abundance of modern (post-1953) groundwater generally decreases with depth and that the abundance of fossil groundwater generally increases with

depth. Topography-driven groundwater flow, geologic layering, and the decrease of permeability with depth generally lead to well-flushed shallow zones overlying poorly-flushed deeper zones, consistent with the occurrence of fossil groundwaters at depth. We conclude that a substantial share (42-85%) of global groundwater in the upper 1 km of the crust is fossil in age. Further, our analysis may even underestimate fossil groundwater abundance because of (a) possible sampling biases towards more permeable basins, (b) contamination of samples by atmospheric $^{14}CO_2$ that would bias our results to smaller fossil groundwater fractions[26], (c) preferential pumping from more permeable strata that may be more likely to contain younger groundwaters (Supplementary Information section S3), and (d) contamination of well waters by recent precipitation due to the construction and use of the well itself (see subsequent section). Although our finding that old water is more common at greater depths is highly intuitive, our analysis is the first global, empirical assessment of the depths at which global aquifer systems transition to poorly-flushed storage dominated by fossil groundwaters.

Global groundwater use is accelerating[27,28] . Declining water tables, more intense droughts, and improved well construction technologies may encourage deeper drilling and increase society's reliance on fossil groundwaters. Assessing how much fossil groundwater is pumped from aquifers requires records of well construction depths, which are available in the western US (Supplementary Information section S4) but not available globally. We examined how frequently fossil groundwaters are pumped in three western US groundwater aquifers by relating constructed well depths to $^{14}C$-based fossil groundwater abundances (Supplementary Information section S4). In the northern High Plains, 99% of wells are shallower than the depth at which fossil groundwaters become common (~170 m), implying that fossil groundwater pumping here is relatively rare (Fig. 3). Similarly, in the San Joaquin Valley, the large majority

(98%) of wells are shallower than the depth at which fossil groundwater becomes common (~240 m). In the Denver Basin, however, many (38%) groundwater wells have been constructed to depths where fossil groundwater is either detectable or dominant (>125 m), implying that fossil groundwater use in the Denver Basin is widespread. Further, fossil groundwater pumping in the Denver Basin has likely increased over the past ~60 years because older wells drilled between 1950 and 1970 were substantially shallower (median well depth of 27 m) than wells constructed more recently than 2010 (median well depth of 126 m), and because total groundwater pumping has more than quadrupled since 1970 (Ref. 29).

Our comparison of groundwater well depths and vertical distributions of fossil groundwater emphasizes that both fossil and post-1953 groundwaters are withdrawn from US aquifers. Pumping fossil groundwater may lead to aquifer depletion, and this risk is greater in arid regions where groundwater tables are deeper and compensatory increases in recharge or decreases in groundwater discharge are less likely (see Ref. 30). Water levels in deep wells have declined across much of the US over the past six decades, likely due to changes in groundwater pumping in response to climate variations[31]. Groundwater well construction is guided by groundwater aquifer conditions (e.g., transmissivity) and quality (e.g., salinity) rather than groundwater age. Nevertheless, we conclude that deep fossil groundwater is already used in some parts of the US, and posit that reliance on fossil groundwaters is probably also widespread in other regions, particularly in hyper-arid climates where modern recharge is negligible.

**Fossil well waters vulnerable to contamination**

Our compilation of radiocarbon and tritium data shows that roughly half of the well water samples that are measurably depleted in carbonate-dissolution-corrected $^{14}C$ (which is clear

evidence of fossil age) also contain measurable amounts of $^{3}H$ (which is unequivocal evidence of recharge after the onset of thermonuclear bomb testing in the 1950s; Table 1). This observation questions the common perception that fossil groundwaters are largely immune to modern contamination (e.g., Refs. 6,7). Our finding that fossil well waters often contain a component of much younger, decades-old groundwater means that fossil well waters—and, possibly, the aquifers from which they derive —are more vulnerable to pollution from modern-era contaminants than previously thought.

*[Table 1 about here]*

Several processes can mix decadal-age groundwater with fossil groundwater and thus make fossil well waters vulnerable to modern contaminants. One plausible explanation is aquifer heterogeneity, leading to preferential flow of younger groundwater through high-permeability zones and slower flows of correspondingly older groundwater through less permeable parts of the aquifer system, with mixing of these different-aged waters by dispersion or diffusion. Topography-driven multi-scale groundwater flow can also result in adjacent groundwater flow paths with very different ages, and thus there can be substantial mixing or dispersion of ages where flow paths converge, such as low-lying discharge areas on the land surface[32,33]. Induced mixing of young and old waters could also occur in wells with open holes or long screens that simultaneously capture young and old groundwater from shallow and deep layers of an aquifer[34,35]. Leaks in corroded or poorly sealed portions of a well may also contribute to mixing of young and old waters in the well bore itself. Co-occurrences of fossil and post-1953 groundwater pumped from wells screened hundreds of meters below the land surface more likely arise from the construction, presence and use of the well itself. For some hydrogeologic settings,

it is unlikely that natural flow paths transmit groundwater hundreds of meters below the land surface within a few decades. We note that tritium occurs equally often in well waters containing some fossil groundwater (tritium was detected in ~half of all samples with >0%) and in well waters containing mostly fossil groundwater (tritium was detected in ~half of samples with >50% fossil water). If natural flow paths were the primary cause of the widespread mixing of fossil and post-1953 groundwater, we would expect that samples dominated by fossil groundwater (>50%) would contain measurable tritium less frequently than samples that contain some fossil groundwater (>0% but possibly <50% fossil water), which is not the case (Table 1). Thus, tritium may co-occur with fossil groundwaters primarily as a result of pumping along extensive well screens, up-coning and down-coning of groundwater due to pumping, and leaks along well bores.

Regardless of how tritium has become mixed with much older groundwaters, the main implication for drinking water supplies is clear: many (~50%) fossil well waters contain detectable amounts of recently recharged groundwater (Table 1), rendering them potentially vulnerable to modern anthropogenic contamination despite their great age. Because aquifers bearing fossil groundwater require millennia to be flushed, their contamination may also persist for millennia, causing effectively irreversible harm to these aquifers over human timescales. However, it remains unclear how frequently tritium arises in fossil well waters as the result of mixing within the aquifer itself, versus mixing induced by the construction and pumping of the groundwater well.

## Concluding remarks

Our analysis shows that fossil groundwater likely dominates global groundwater storage in the uppermost 1 km of the crust (42-85%). This figure is likely to be a lower bound on the global prevalence of groundwater, because the likely biases in our analysis (detailed above) serve to minimize our calculated fossil groundwater fractions. Further, our analysis focuses solely on the shallowest 1 km of the crust that is also the most rapidly flushed. Fractured rocks deeper than 1 km can host ancient fossil groundwaters that have been isolated for millions or even billions of years[36-37].

Improving access to freshwater for agriculture, households, and industry while sustaining vital ecosystems in a changing global environment represents a critical scientific and political challenge. Fossil groundwater resources likely comprise more than half of global unfrozen freshwater (Figs. 1 and 2), and dependence upon fossil groundwater to meet water demands is rising as a consequence of increasing groundwater withdrawals and deeper drilling in some regions (e.g., Denver Basin, USA). Groundwater quality remains a critical concern in many parts of the world[38-41], and our results highlight that even though deeper wells pump predominantly fossil groundwater, they are not immune to modern contamination.

## Methods

### Global groundwater isotope data.

We analysed global groundwater isotope data compiled from hundreds of primary literature sources and from the United States Geological Survey's Water Quality Portal (Tables S1 and S2). About two-thirds (65%) of our global radiocarbon compilation comes from North America, which represents only ~18% of the global landmass. By contrast, only 9% and 11% of our compiled radiocarbon data come from Africa and Asia, which each comprise much larger

shares of global ice-free land areas (~22% and ~33% of the global landmass, respectively; Fig. S2). We analysed the compiled groundwater isotope data to partition the fraction of groundwater samples that recharged (i) before the Holocene-Pleistocene transition 11,700 years ago ("fossil groundwater", based on $^{14}C$ with a half-life of 5730 years), and (ii) more recently than 1953, when the "hydrogen bomb peak" in meteoric tritium began ("post-1953 groundwater", based on $^{3}H$ with a half-life of 12.3 years).

**Determining fossil groundwater fractions.**

We used stable ($\delta^{13}C$) and radioactive ($^{14}C$) carbon isotope data to calculate fossil groundwater fractions ($F_{fossil}$) following (Ref. 20):

$$F_{Fossil} = 1 - \frac{^{14}C_{sample} - ^{14}C_{fossil}}{^{14}C_{Holocene} - ^{14}C_{fossil}} \qquad \textit{Equation 1}$$

where dissolved inorganic carbon concentrations are assumed to be roughly equal for the fossil and Holocene waters[20], and $^{14}C$ represents the radiocarbon activity of: the groundwater sample (subscript "sample"), Holocene groundwater recharged within the past 11,700 years (subscript "Holocene"), or fossil groundwater recharged more than 11,700 years ago (subscript "fossil"). Holocene and fossil $^{14}C$ inputs are based on late-Quaternary atmospheric $^{14}C$ time series[42,43] corrected for radioactive decay following (Ref. 20):

$$^{14}C_t = \left(q_t \, ^{14}C_{precip(t)} e^{-0.693(t_{sample} - t)/(5730\ years)}\right)_t \qquad \textit{Equation 2}$$

where $^{14}C_{precip(t)}$ represents precipitation $^{14}C$ at time $t$, and $t_{sample}$ is the date that the groundwater sample was analysed. $^{14}C_{Holocene}$ is represented by $^{14}C_t$ evaluated for the time interval of $0 < \text{abs}(t_{sample} - t) < 11700$ years; $^{14}C_{fossil}$ is represented by $^{14}C_t$ evaluated prior to the Holocene (i.e., $\text{abs}(t_{sample} - t) > 11700$ years). For years postdating thermonuclear-bomb testing, we apply a 10-

year running average to estimate the maximum possible $^{14}C_{Holocene}$ value (Supplementary Fig. S5), effectively assuming some amount of dispersion has taken place in most aquifer systems over the past 50 years. The factor $q$ is used to correct for the dissolution of carbonate with zero radiocarbon:

$$q_t = \frac{\delta^{13}C_t - \delta^{13}C_{carbonate}}{\delta^{13}C_{recharge} - \delta^{13}C_{carbonate}} \qquad \textit{Equation 3}$$

where $\delta^{13}C_{recharge}$ and $\delta^{13}C_{carbonate}$ are the stable isotope compositions of recharge and carbonates. We used $\delta^{13}C_{recharge}$ and $\delta^{13}C_{carbonate}$ values reported in the compiled studies when available, and otherwise assumed[20] $\delta^{13}C_{carbonate} = 0$ ‰ and $\delta^{13}C_{recharge} = -14.3$ ‰. Global $\delta^{13}C_{carbonate}$ and $\delta^{13}C_{recharge}$ values vary around the globe[20] such that our assumption of $\delta^{13}C_{carbonate} = 0$ ‰ and $\delta^{13}C_{recharge} = -14.3$ ‰ introduces uncertainty into our fossil groundwater calculations.

The range of $\delta^{13}C$ values ascribed to each time interval ($\delta^{13}C_t$) is assumed to be constrained by $\delta^{13}C_{recharge} \leq \delta^{13}C_{Holocene} \leq \delta^{13}C_{sample} \leq \delta^{13}C_{fossil} \leq \delta^{13}C_{carbonate}$ (Ref. 20). Because the possible ages of the Holocene and pre-Holocene end members vary widely, the ranges of $^{14}C_{Holocene}$ and $^{14}C_{fossil}$ values are often large; we apply upper and lower limits of $^{14}C_{Holocene}$ and $^{14}C_{fossil}$ in equation 1 to estimate minimum and maximum fossil groundwater fractions. $^{14}C_{Holocene}$ and $^{14}C_{fossil}$ share an identical end-member at the 11,700 year boundary. The shared 11.7 ka endmember, and the large atmospheric radiocarbon variations over each end-member interval, lead to highly uncertain $F_{fossil}$ calculations for some samples.

In each aquifer, we pinpointed two depths where we observed transitions from Holocene groundwater to pre-Holocene fossil groundwater, and used these depths as upper and lower limits in the bar graphs shown in Fig. 1. The first (shallower) recorded transition depth specifies

a depth below which the majority (>50%) of well water samples from a given aquifer must contain some fraction of fossil groundwater (i.e., over half the samples have a minimum fossil groundwater fraction of greater than zero). The second (deeper) recorded transition depth represents a depth below which the majority (>50%) of sampled well waters from a given aquifer system must contain mostly fossil groundwater (i.e., over half of the samples deeper than the depth have a minimum fossil groundwater fraction of greater than 50%).

Where oxygen stable isotope data are also available, we confirmed the depth to fossil groundwater by comparing the $^{18}O/^{16}O$ ratio in groundwater to a new global map of $\delta^{18}O$ in late-Pleistocene precipitation[44]; where $\delta^{18}O = ([^{18}O/^{16}O_{\text{sample}}] / [^{18}O/^{16}O_{\text{standard ocean water}}] - 1) \times 10^3$ ‰. Late-Holocene and late-Pleistocene precipitation $\delta^{18}O$ values are detectably different (>1 ‰) over the great majority (~87%) of the global landmass[44], enabling use of depth-$\delta^{18}O$ plots as a qualitative secondary indicator of the depth to fossil groundwater.

**Determining post-1953 groundwater fractions.**

To calculate the fraction of modern, post-1953 groundwater in a sample we used globally-interpolated precipitation tritium for years spanning the pre-bomb era (prior to 1950) to 2010 from Ref. 24. Global precipitation $^3H$ estimates derive from >60,000 monthly $^3H$ measurements made at 738 globally distributed stations (data provided by the International Atomic Energy Agency: iaea.org/water). We then weighted the monthly precipitation $^3H$ data against the long-term average monthly precipitation rate[45] to estimate an annually integrated precipitation $^3H$ value at each well site. Once a precipitation tritium record was developed for each well location (from Ref. 24), we decay-corrected the precipitation tritium input curve to the date that each sample was collected[20]. As in our radiocarbon-based calculation, we assume that

some amount of dispersion takes place in the aquifer and apply a 10-year running average before calculating maximum and minimum possible ${}^{3}H_{post\text{-}1953}$ values (Supplementary Fig. S5). We then applied the range of possible decay-corrected, post-1953 precipitation $^{3}$H values as one end-member in a two-component mixing model, and pre-1953 precipitation $^{3}$H as the other component:

$$F_{post-1953} = \frac{{}^{3}H_{sample} - {}^{3}H_{pre-1953}}{{}^{3}H_{post-1953} - {}^{3}H_{pre-1953}} \qquad \textit{Equation 4}$$

where ${}^{3}H_{sample}$ is the measured $^{3}$H in the groundwater sample, and ${}^{3}H_{pre\text{-}1953}$ and ${}^{3}H_{post\text{-}1953}$ are the local meteoric water tritium activities that have been decay-corrected to the time of sampling for either (i) prior to 1953 (${}^{3}H_{pre\text{-}1953}$), or years after 1953 (${}^{3}H_{post\text{-}1953}$). The year 1953 was selected as a threshold[20] so that the overwhelming majority of possible ${}^{3}H_{pre\text{-}1953}$ values fall below analytical detection limits, leading us to assume ${}^{3}H_{pre\text{-}1953} \approx 0$. We assume subterranean tritium production leads to secular equilibrium tritium contents that do not exceed the common analytical detection limit of 0.8 tritium units.

**Estimating groundwater age-storage volumes.**

In Fig. 2 of the main text, we present ranges of fossil and post-1953 groundwater with depth. The ranges shown represent averages of the minimum and maximum fossil groundwater (or post-1953 groundwater) fractions at each depth interval. For example, the range of fossil groundwater from 0 m to 25 m depth shown in Fig. 2a is 3%-52%, where 3% is the average minimum fossil groundwater fractions among all n=627 wells screened in the uppermost 25 m of the crust, and 52% is the average maximum fossil groundwater fraction for these n=627 well waters.

## Data availability

Compiled isotope data are available in the primary references listed in Tables S1 and S2 and in tabulated form from www.isohydro.ca.

## Acknowledgements

This project was supported by an NSERC Discovery Grant to S.J. (no. 5668).

## Contributions

S.J. and J.W.K. analysed the compiled groundwater isotope data and wrote initial drafts of the manuscript. S.J. and D.P. analysed the compiled groundwater well construction data. All authors discussed results and edited the manuscript.

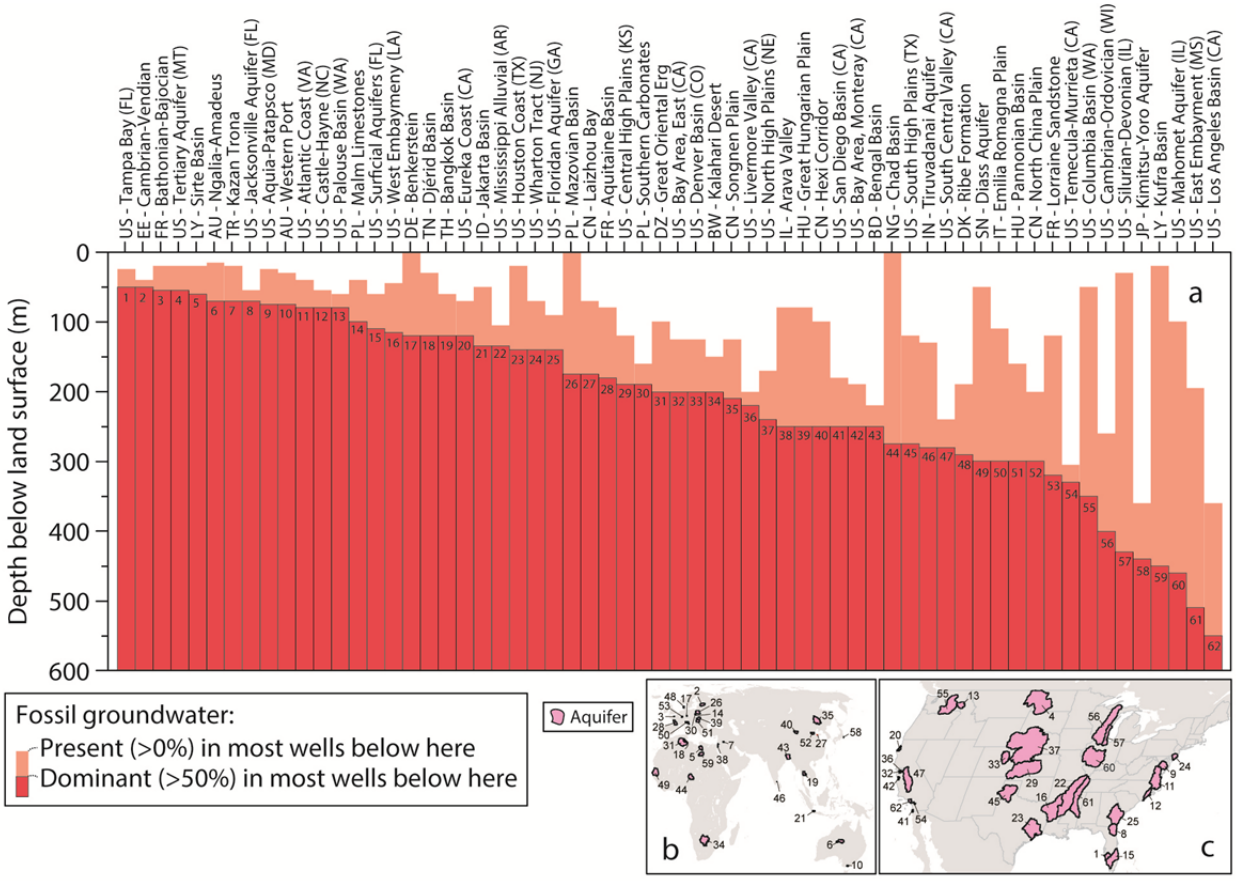


341

342 **Fig. 1.** Prevalence of fossil groundwater in global aquifers. (a) Depth to the fossil groundwater
343 transition in 62 aquifers. The shallow depth (top of orange bar) represents a depth below which
344 most wells (>50%) contain detectable fossil groundwater (minimum fossil groundwater fraction
345 >0%). The deeper depth (top of red bar) represents a depth below which most wells (>50%) are
346 dominated by fossil groundwater (minimum fossil groundwater fraction is >50%). Fossil
347 groundwater becomes dominant at a median depth of 200 m, an upper-lower quartile range of
348 depths of 115-290 m, and a $10^{th}$-$90^{th}$ percentile range of depths of 70-430 m. We note that the
349 lower limit of our graph (600 m) does not necessarily represent the lower boundary for any of
350 our 62 study aquifers, nor do the depths covered by red and orange bars imply that the
351 groundwater quality is high or that the aquifer is productive at these depths.

352

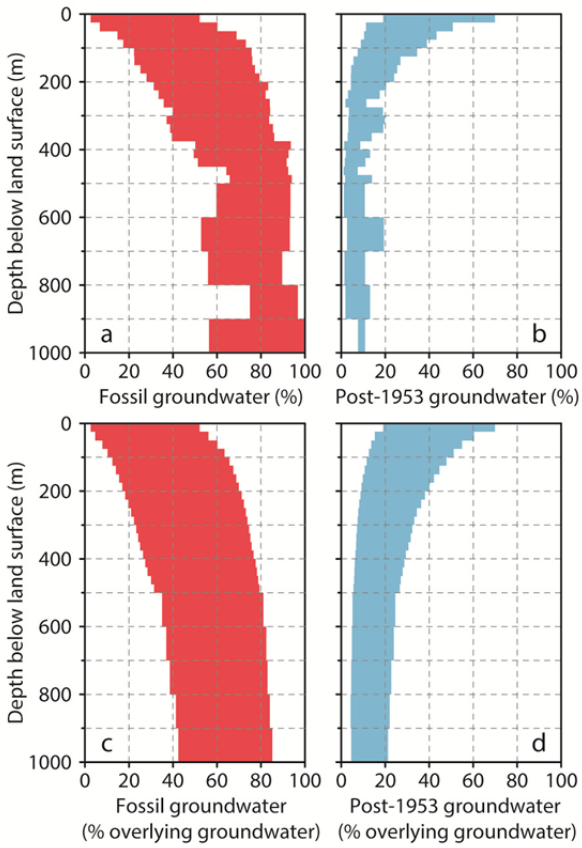


353

354 **Fig. 2.** Variations of fossil (red) and post-1953 groundwater (blue) with depth. Panels a and b
355 show statistical distributions of fossil and post-1953 groundwater binned at various depths.
356 Panels c and d show the cumulative distribution with depth of stored fossil groundwater (pre-
357 Holocene; red in panel a) and modern groundwater (post-1953; blue in panel b); that is, these
358 panels represent the fraction of total groundwater overlying a given depth (data have been
359 corrected for porosity changes with depth following Ref. 1). The coloured areas represent the
360 estimated maximum and minimum range, calculated using all groundwater samples within a
361 given depth bin (average of the maximum and minimum estimates of fossil groundwater and
362 post-1953 groundwater for a given range of well depths).

363

364 **Table 1.** Radioisotope ($^{14}C$, $^{3}H$) evidence for post-1953 and fossil groundwater mixing

| Presence of fossil groundwater | Total $^{14}C$ samples with $^{3}H$ data | Presence of post-1953 groundwater | |
|---|---|---|---|
| | | Present ($^{3}H>0$) | Absent ($^{3}H\approx0$) |
| May contain no fossil water (possibly 0%) | n=984 | 74% | 26% |
| Must contain fossil water (>0% and possibly <50%) | n=179 | 49% | 51% |
| Must contain mostly fossil water (>50%) | n=365 | 50% | 50% |

365

## References


1. Gleeson, T., Befus, K. M., Jasechko, S., Luijendijk, E. & Cardenas, M. B. The global volume and distribution of modern groundwater. *Nature Geoscience* **9,** 161–168 (2016).
2. Messager, M. L., Lehner, B., Grill, G., Nedeva, I. & Schmitt, O. Estimating the volume and age of water stored in global lakes using a geo-statistical approach. *Nature Communications* **7,** 13603 (2016).
3. Siebert, S., Burke, J., Faures, J. M., Frenken, K., Hoogeveen, J., Döll, P., & Portmann, F. T. Groundwater use for irrigation–a global inventory. *Hydrol. Earth Syst. Sci.* **14** 1863–1880 (2010).
4. Fan, Y., Li, H., & Miguez-Macho, G. Global patterns of groundwater table depth. *Science* **339,** 940–943 (2013).
5. Chen, Z., Nie, Z., Zhang, Z., Qi, J. & Nan, Y. Isotopes and sustainability of ground water resources, North China Plain. *Groundwater* **43,** 485–493 (2005).
6. Yamada, C. First report on shared natural resources, United Nations International Law Commission, A/CN.4/533 + Add.1 (2003), access from: legal.un.org/ilc/documentation/english/a_cn4_533.pdf
7. Buser, H. R. Atrazine and other s-triazine herbicides in lakes and in rain in Switzerland. *Environ. Sci. Technol.* **24,** 1049–1058 (1990).
8. Burgess, W. G., Hoque, M. A., Michael, H. A., Voss, C. I., Breit, G. N. & Ahmed, K. M. (2010). Vulnerability of deep groundwater in the Bengal Aquifer System to contamination by arsenic. *Nature Geoscience* **3,** 83–87 (2010).
9. Taylor, R. G. et al. Ground water and climate change. *Nat. Clim. Change* **3,** 322–329 (2013).
10. Thatcher, L., Rubin, M. & Brown, G. F. Dating desert groundwater. *Science* **134,** 105–106 (1961).
11. Edmunds, W. M. & Wright, E. P. Groundwater recharge and palaeoclimate in the Sirte and Kufra basins, Libya. *J. Hydrol.* **40,** 215–241 (1979).
12. Phillips, F. M., Peeters, L. A., Tansey, M. K. & Davis, S. N. Paleoclimatic inferences from an isotopic investigation of groundwater in the central San Juan Basin, New Mexico, *Quatern. Res.* **26,** 179–193 (1986).

13. Weyhenmeyer, C. E., Burns, S. J., Waber, H. N., Aeschbach-Hertig, W., Kipfer, R., Loosli, H. H. & Matter, A. Cool glacial temperatures and changes in moisture source recorded in Oman groundwaters. *Science* **287,** 842–845 (2000).
14. Plummer, N. L. & Sprinkle, C. L. Radiocarbon dating of dissolved inorganic carbon in groundwater from confined parts of the Upper Floridan aquifer, Florida, USA. *Hydrogeol. J.* **9,** 127-150 (2001).
15. Vengosh, A., Gill, J., Davisson, M. L. & Hudson, G. B. A multi-isotope (B, Sr, O, H, and C) and age dating ($^{3}$H–$^{3}$He, and $^{14}$C) study of groundwater from Salinas Valley, California: Hydrochemistry, dynamics, and contamination processes. *Water Resour. Res.* **38,** 1008 (2002).
16. Brown, K. B., McIntosh, J. C., Baker, V. R. & Gosch, D. Isotopically-depleted late Pleistocene groundwater in Columbia River Basalt aquifers: Evidence for recharge of glacial Lake Missoula floodwaters? *Geophys. Res. Lett.* **37,** L21402 (2010).
17. Morrissey, S. K., Clark, J. F., Bennett, M., Richardson, E. & Stute, M. Groundwater reorganization in the Floridan aquifer following Holocene sea-level rise. *Nature Geoscience* **3,** 683–687 (2010).
18. Cartwright, I. & Weaver, T. R. Hydrogeochemistry of the Goulburn Valley region of the Murray Basin, Australia: implications for flow paths and resource vulnerability. *Hydrogeol. J.* **13,** 752-770 (2005).
19. Vogel, J. C. Carbon-14 dating of groundwater. Isotope Hydrology. International Atomic Energy Agency STI/PUB/255, 225–239 (1970).
20. Jasechko, S. Partitioning young and old groundwater with geochemical tracers. *Chem. Geol.* **427,** 35–42 (2016a).
21. Weissmann, G. S., Zhang, Y., LaBolle, E. M. & Fogg, G. E. Dispersion of groundwater age in an alluvial aquifer system. *Water Resour. Res.* **38,** 1198 (2002).
22. Bethke, C.M. and Johnson, T.M., 2008. Groundwater age and groundwater age dating. *Annu. Rev. Earth Planet. Sci.* 36, 121–152.
23. Torgersen, T., Purtschert, R., Phillips, F. M., Plummer, L. N., Sanford, W. E. & Suckow, A. Defining groundwater age. in: Isotope Methods for Dating Old Groundwater, International Atomic Energy Agency, Vienna, Austria (2013).

24. Jasechko, S. & Taylor, R. G. Intensive rainfall recharges tropical groundwaters. *Environ. Res. Lett.* **10,** 124015 (2015).
25. Jasechko, S., Kirchner, J. W., Welker, J. M. & McDonnell, J. J. Substantial proportion of global streamflow less than three months old. *Nature Geoscience* **9,** 126–129 (2016).
26. Aggarwal, P. K., Araguas-Araguas, L., Choudhry, M., van Duren, M. & Froehlich, K. Lower groundwater $^{14}C$ age by atmospheric $CO_2$ uptake during sampling and analysis. *Groundwater* **52,** 20–24 (2014).
27. Wada, Y., Wisser, D. & Bierkens, M. F. P. Global modeling of withdrawal, allocation and consumptive use of surface water and groundwater resources. *Earth System Dynamics* **5,** 1-15 (2014).
28. Famiglietti, J. S. The global groundwater crisis. *Nature Climate Change* **4,** 945-948 (2014).
29. Bauch, N. J., Musgrove, M., Mahler, B. J. & Paschke, S. S. Water Quality in the Denver Basin Aquifer System, Colorado, 2003-05, pp. 113 (2014).
30. Theis, C. V. The source of water derived from wells. *Civil Eng*. **10,** 277–280 (1940).
31. Russo, T.A. & Lall, U. Depletion and response of deep groundwater to climate-induced pumping variability. *Nature Geoscience,* doi:10.1038/ngeo2883 (2017).
32. Toth, J. A theoretical analysis of groundwater flow in small drainage basins. *J. Geophys. Res.* **68,** 4795–4812 (1963).
33. Jiang, X. W., Wan, L., Cardenas, M. B., Ge, S. & Wang, X. S. Simultaneous rejuvenation and aging of groundwater in basins due to depth-decaying hydraulic conductivity and porosity. *Geophys. Res. Lett.* **37,** L05403 (2010).
34. Zinn, B. A., & Konikow, L. F. Effects of intraborehole flow on groundwater age distribution. *Hydrogeol. J.* **15,** 633-643 (2007).
35. Ferguson, G. A., Betcher, R. N. and Grasby, S. E. Hydrogeology of the Winnipeg formation in Manitoba, Canada. *Hydrogeol J.* **15,** 573–587 (2007).
36. Lin, L. H. et al. Long-term sustainability of a high-energy, low-diversity crustal biome. *Science* **314,** 479-482 (2006).
37. Holland, G., Sherwood Lollar, B., Li, L., Lacrampe-Couloume, G., Slater, G. F. & Ballentine, C. J. Deep fracture fluids isolated in the crust since the Precambrian. *Nature* **497,** 367-360 (2013).

38. Burow, K. R., Nolan, B. T., Rupert, M. G. & Dubrovsky, N. M. Nitrate in groundwater of the United States, 1991−2003. *Environmental Science & Technology* **44,** 4988-4997 (2010).
39. Graham, J. P. & Polizzotto, M. L. Pit latrines and their impacts on groundwater quality: A systematic review. *Environmental Health Perspectives* **121** (2013).
40. Sorensen, J. P. R. et al. Emerging contaminants in urban groundwater sources in Africa. *Water Research* **72,** 51-63 (2015).
41. MacDonald, A. M. et al. Groundwater quality and depletion in the Indo-Gangetic Basin mapped from in situ observations. *Nature Geoscience* **9,** 762–766 (2016).
42. Reimer, P. J. et al. IntCal13 and Marine13 radiocarbon age calibration curves 0–50,000 years cal BP. *Radiocarbon* **55,** 1869–1887 (2013).
43. Hua, Q. & Barbetti, M. Review of tropospheric bomb $^{14}C$ data for carbon cycle modeling and age calibration purposes. *Radiocarbon* **46,** 1273–1298 (2004).
44. Jasechko, S. Late-Pleistocene precipitation $\delta^{18}O$ interpolated across the global landmass. *Geochem. Geophys. Geosy.* **17,** 3274–3288 (2016b).
45. New, M., Lister, D., Hulme, M. & Makin, I. A high-resolution data set of surface climate over global land areas. *Climate Research* **21,** 1–25 (2002).

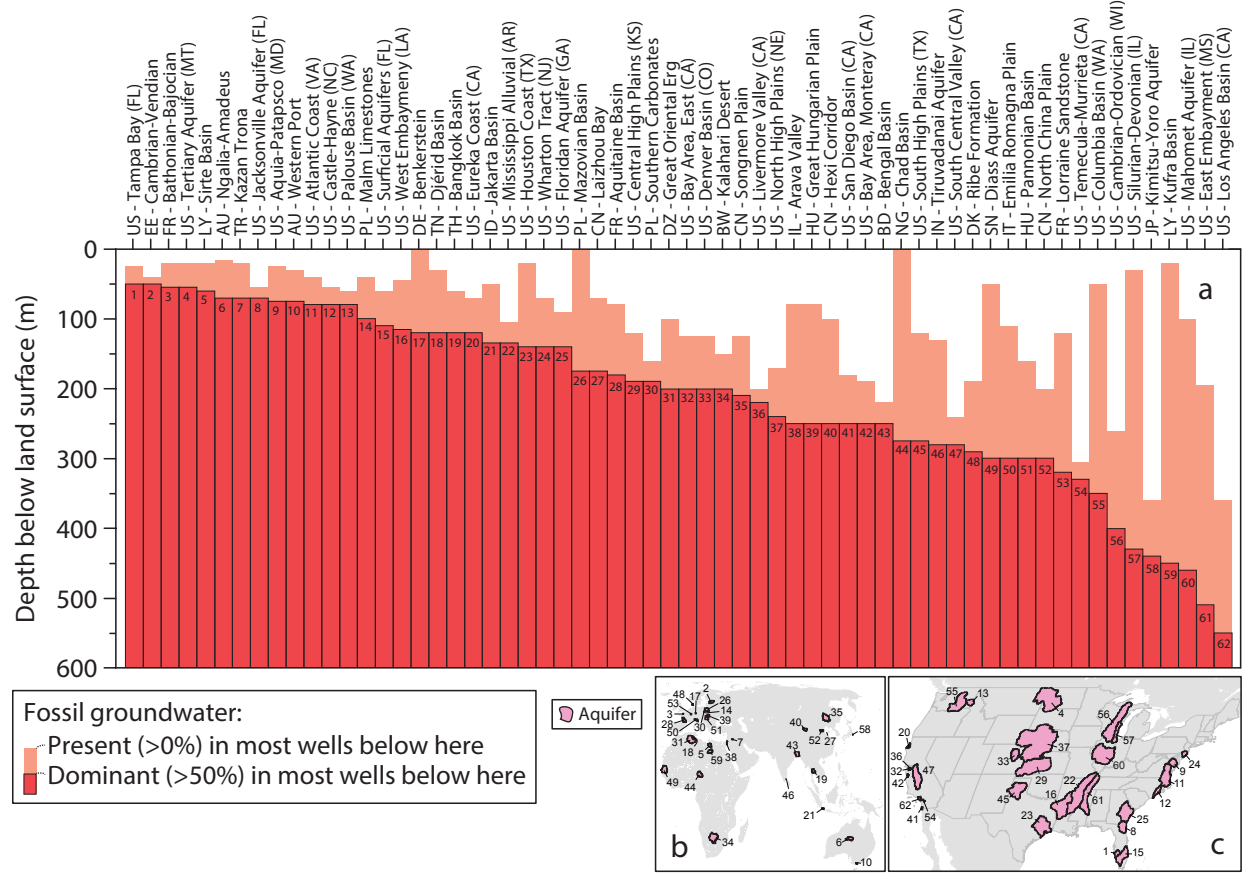
US - Tampa Bay (FL)
EE - Cambrian-Vendian
FR - Bathonian-Bajocian
US - Tertiary Aquifer (MT)
LY - Sirte Basin
AU - Ngalia-Amadeus
TR - Kazan Trona
US - Jacksonville Aquifer (FL)
US - Aquia-Patapsco (MD)
AU - Western Port
US - Atlantic Coast (VA)
US - Castle-Hayne (NC)
US - Palouse Basin (WA)
PL - Malm Limestones
US - Surficial Aquifers (FL)
US - West Embayment (LA)
DE - Benkerstein
TN - Djérid Basin
TH - Bangkok Basin
US - Eureka Coast (CA)
ID - Jakarta Basin
US - Mississippi Alluvial (AR)
US - Houston Coast (TX)
US - Wharton Tract (NJ)
US - Floridan Aquifer (GA)
PL - Mazovian Basin
CN - Laizhou Bay
FR - Aquitaine Basin
US - Central High Plains (KS)
PL - Southern Carbonates
DZ - Great Oriental Erg
US - Bay Area, East (CA)
US - Denver Basin (CO)
BW - Kalahari Desert
CN - Songnen Plain
US - Livermore Valley (CA)
US - North High Plains (NE)
IL - Arava Valley
HU - Great Hungarian Plain
CN - Hexi Corridor
US - San Diego Basin (CA)
US - Bay Area, Monteray (CA)
BD - Bengal Basin
NG - Chad Basin
US - South High Plains (TX)
IN - Tiruvadanai Aquifer
US - South Central Valley (CA)
DK - Ribe Formation
SN - Diass Aquifer
IT - Emilia Romagna Plain
HU - Pannonian Basin
CN - North China Plain
FR - Lorraine Sandstone
US - Temecula-Murrieta (CA)
US - Columbia Basin (WA)
US - Cambrian-Ordovician (WI)
US - Silurian-Devonian (IL)
JP - Kimitsu-Yoro Aquifer
LY - Kufra Basin
US - Mahomet Aquifer (IL)
US - East Embayment (MS)
US - Los Angeles Basin (CA)
Depth below land surface (m)
0
100
200
300
400
500
600
a
Fossil groundwater:
Present (>0%) in most wells below here
Dominant (>50%) in most wells below here
Aquifer
b
c

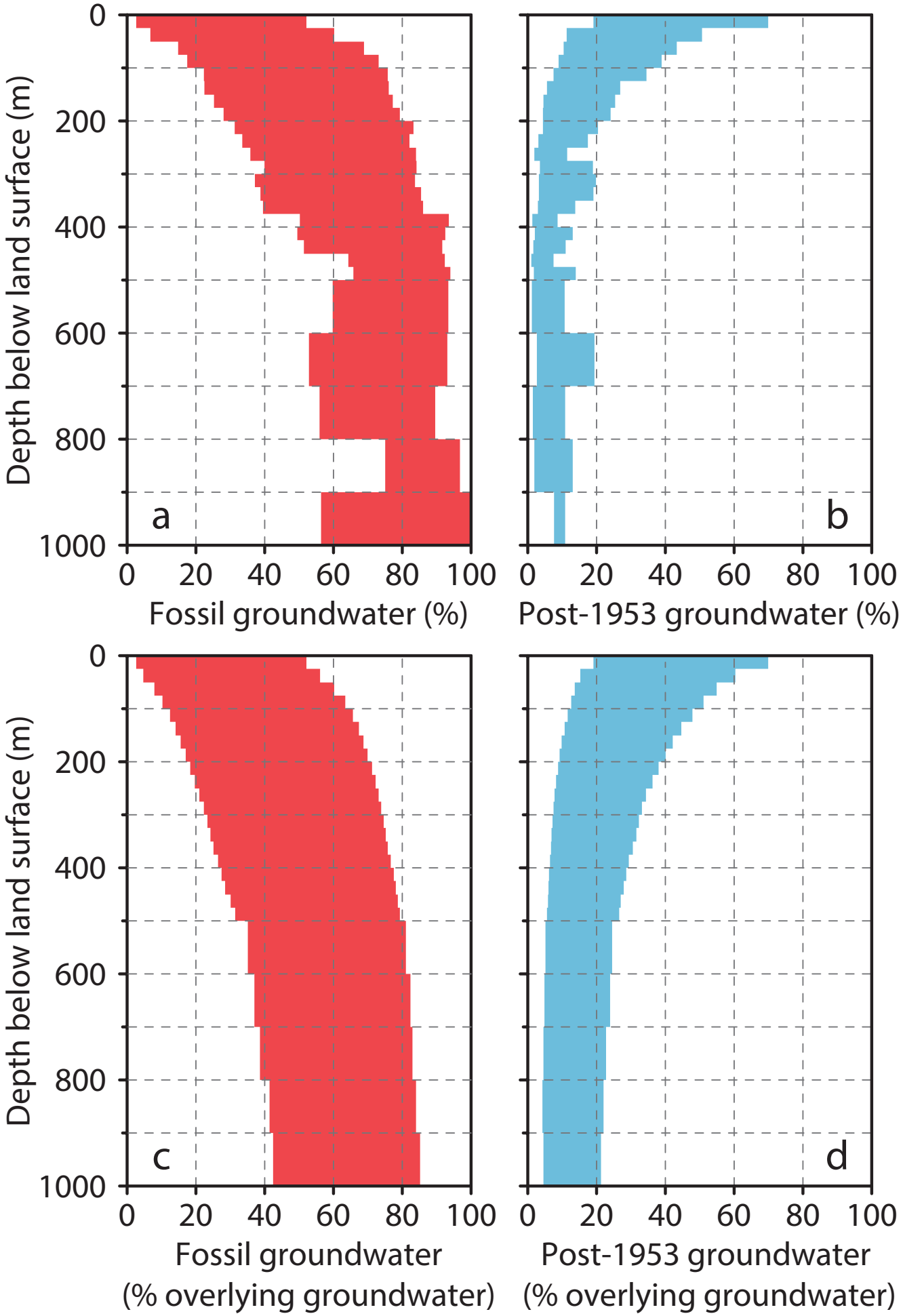
Depth below land surface (m)
0
200
400
600
800
1000
a
0
20
40
60
80
100
Fossil groundwater (%)
b
Post-1953 groundwater (%)
c
Fossil groundwater
(% overlying groundwater)
d
Post-1953 groundwater
(% overlying groundwater)